

Amperometric and Impedimetric Determination of Hydrazine at a Novel Trimethine Cyanine Dye Film Modified Glassy Carbon Electrode

Jia-Xuan Wei¹, Arun Prakash Periasamy¹, and Shen-Ming Chen^{1,*}

¹Department of Chemical Engineering and Biotechnology, National Taipei University of Technology, No.1, Section 3, Chung-Hsiao East Road, Taipei 106, Taiwan (ROC).

*E-mail: smchen78@ms15.hinet.net

Received: 9 May 2011 / Accepted: 4 June 2011 / Published: 1 July 2011

In this study, we report the amperometric and impedimetric determination of hydrazine at a novel trimethine cyanine dye, 1H-Benz[e]indolium, 2-[3-(3-butyl-1, 3-dihydro-1, 1-dimethyl-2H-benz[e]indol-2-ylidene)-1-propenyl]-1, 1, 3-trimethyl-, hexafluorophosphate (DVD-R dye A4) or (DVDR) film modified glassy carbon electrode (GCE). The DVDR film was electrochemically deposited on a GCE surface by performing 20 consecutive cyclic voltammograms at the scan rate of 100 mV s⁻¹ in the potential range between -0.8 and 2.0 V in 0.1 mM DVDR in 0.1 M H₂SO₄ solution. The SEM and AFM results revealed that DVDR film surface possess both flake and bead like structures. Cyclic voltammetry (CV) results demonstrated that DVDR film was electrochemically active and it showed a pair of well-defined redox peaks at a formal potential (E^{o'}) of 5.5 mV in pH 7. Electrochemical impedance spectroscopy (EIS) results showed that rapid electron transfer process occurs at the DVDR/GCE surface than the bare/GCE surface. The electron transfer resistance (R_{et}) values obtained at the DVDR film increased linearly with increase in hydrazine concentrations between 0.05 mM–1.07 mM, which confirmed the excellent impedimetric hydrazine quantification. The DVDR film showed rapid amperometric i-t response towards hydrazine in the linear concentration range between 1 x 10⁻⁶ M–2.22 x 10⁻⁴ M with a sensitivity of 0.571 μA μM⁻¹ cm⁻² of hydrazine. Even though large amounts (1000/500-fold) of the common cations/anions coexist in the same supporting electrolyte, they do not produce any notable interference effect with the hydrazine oxidation signal, which validates the high selectivity of DVDR film for hydrazine. Moreover, acceptable recovery was achieved at the DVDR/GCE in hydrazine spiked various water samples, which confirmed the practical applicability of the developed sensor.

Keywords: Trimethine cyanine dyes, conducting film, hydrazine, impedimetric detection, amperometry.

1. INTRODUCTION

Cyanine dyes belong to the class of organic dyes which contain two heterocyclic nitrogen atoms joined by a conjugated chain of carbon atoms [1]. The most common heterocyclic components found in cyanine dyes include quinoline, indole, benzoxale and benzothiazole [2]. The cyanine dyes can be classified into mono, tri and heptamethine cyanine dyes based on the number of methine groups connecting the heterocyclic rings. So far, based on the versatile approaches used by many research groups, several preparation methods have been reported for monomethine [3], trimethine [4–6] and heptamethine cyanine dyes [7]. In recent years, cyanine dyes have attracted considerable attention and they have been widely employed to determine the antibacterial activity [8], as fluorescent probes [9], in histology as a stain for nucleic acids, proteins, polysaccharides, and lipids [10], for solar cells [11, 12], optics [13], photovoltaics [14] and photographic [15] applications. In the electrochemistry point of view, cyanine dyes are electrochemically active and earlier Netzel *et al.* have reported the redox potentials of several cyanine dyes [16]. Owing to the excellent properties and wide applications of cyanine dyes, in the present study we attempted to study the electrochemical activity of a trimethine cyanine dye, 1H-Benz[e]indolium, 2-[3-(3-butyl-1, 3-dihydro-1, 1-dimethyl-2H-benz[e]indol-2-ylidene)-1-propenyl]-1, 1, 3-trimethyl-, hexafluorophosphate (DVD-R dye A4) or (DVDR). The structure of DVDR is shown in Fig. 1.

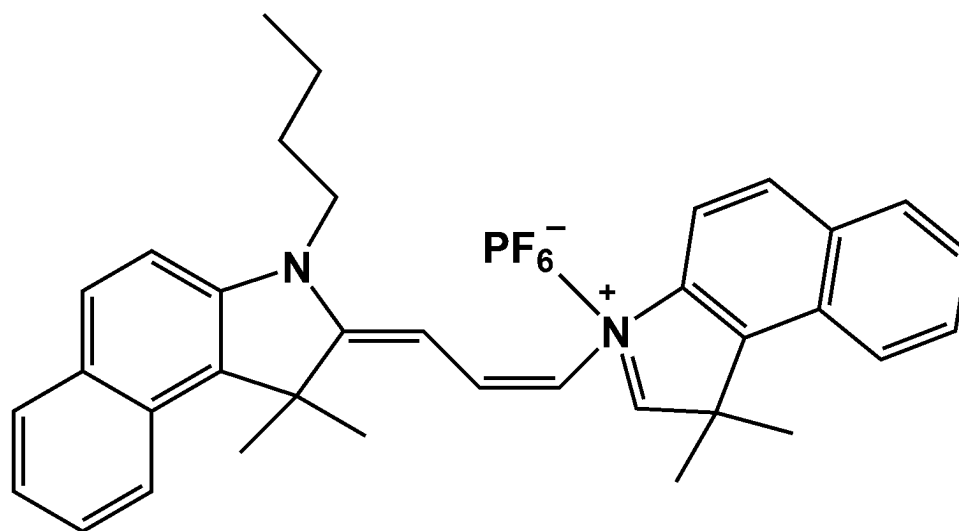


Figure 1. Structure of DVDR dye A4.

We electrochemically deposited the DVDR dye on a glassy carbon electrode (GCE). This kind of green approach avoids the use of hazardous additives and tedious instrumentation techniques for preparing thin film of trimethine cyanine dyes on the electrode surface, which could encourage their electrochemical applications.

On the other hand, hydrazine is a strong reducing agent and it reacts readily and exothermically with most oxidizing agents. Owing to the high reactivity of hydrazine, it has been extensively employed for various industrial [17] and fuel cell applications [18]. However, hydrazine is highly toxic

and acute exposure to high levels of hydrazine may cause drastic effects in humans and animals [19]. In particular, because of its carcinogenic and hepatotoxic activity, hydrazine affects the liver and brain glutathione and hence serious attention has been focused towards hydrazine detection [20]. However, the conventional methods used for hydrazine detection involve tedious instruments and are rather time consuming [21, 22]. In contrast, the electrochemical approaches are rapid and they provide high sensitivity and selectivity for hydrazine quantification. However, the important shortcoming in electrochemical measurements is the unmodified electrodes often requires large overpotential for hydrazine oxidation [23] and this may cause serious electrode fouling and interference effect due to the oxidation of coexisting common ions. This shortcoming was overcome by the utilization of modified electrodes in hydrazine determination, which considerably lowered the over potential for hydrazine oxidation with high sensitivity and selectivity [24–29].

In the present study, we report the amperometric and impedimetric determination of hydrazine at a novel conducting trimethine cyanine dye, DVDR film modified GCE. The modified electrode shows excellent catalytic activity towards hydrazine with high sensitivity and selectivity. Moreover, compared with unmodified electrode, the DVDR film modified GCE considerably lowers the overpotential for hydrazine oxidation. The practical applicability of the proposed method has also been evaluated by the detection of hydrazine from various water samples with acceptable recovery.

2. EXPERIMENTAL

2.1. Reagents

1H-Benz[e]indolium, 2-[3-(3-butyl-1, 3-dihydro-1, 1-dimethyl-2H-benz[e]indol-2-ylidene)-1-propenyl]-1, 1, 3-trimethyl-, hexafluorophosphate (DVD-R dye A4) or (DVDR) was obtained from an organic dyes manufacturing company in Taiwan. Hydrazine sulfate was purchased from Hayashi pure chemical industries Ltd. Japan.

The supporting electrolytes used for electrochemical studies were either 0.1 M H₂SO₄ or 0.05 M pH 7 phosphate buffer solution (PBS). PBS was prepared using 0.05 M Na₂HPO₄ and NaH₂PO₄ solutions. All the reagents used in this work were of analytical grade and all aqueous solutions were prepared using doubly distilled water. Prior to each experiment, the experimental solutions were deoxygenated with pre-purified N₂ gas for 10 min and the N₂ tube was kept above the solutions to maintain an inert atmosphere.

2.2. Apparatus

Cyclic voltammetry (CV) experiments were carried out using CHI 1205a work station. A conventional three electrode cell containing 4 ml of 0.1 M H₂SO₄ or PBS was used for electrochemical studies. GCE with an electrode surface area of 0.079 cm² was used as working electrode. Pt wire with 0.5 mm diameter was used as counter electrode and all the potentials were referred with respect to standard Ag/AgCl reference electrode. Amperometric (i-t curve) measurements were performed using

CHI 750 potentiostat with analytical rotator AFMSRX (PINE Instruments, USA). EIM6ex ZAHNER (Kroanch, Germany) was used for electrochemical impedance spectroscopy (EIS) and impedimetric catalysis experiments. Surface morphological studies were carried out using Hitachi S-3000 H scanning electron microscope (SEM) and Being nano-instruments CSPM 4000, atomic force microscope (AFM).

2.3. Electrochemical deposition of DVDR film on GCE by cyclic voltammetry

The GCE surface was polished to a mirror finish on a clean Buehler polishing cloth using 0.05 μm alumina slurry. In order to remove the loosely adsorbed alumina particles the polished GCE surface was washed and ultrasonicated in doubly distilled water for 10 min. Finally, the clean GCE surface was dried in air for few min and it was transferred to an electrochemical cell containing 0.1 mM DVDR dye in 0.1 M H_2SO_4 solution. The DVDR film was electrochemically deposited on the clean GCE surface by performing 20 consecutive cyclic voltammograms at the scan rate of 100 mV s^{-1} in the potential range between -0.8 and 2.0 V (see Fig. 2). The DVDR dye concentration and the potential range mentioned above were optimized based on the uniform film growth and the occurrence of well defined redox peaks.

We have also optimized the DVDR film deposition cycles. After performing 5, 10, 15 and 20 film deposition cycles, the DVDR film modified GCE was gently washed with water and the cyclic voltammograms were recorded in the potential range between -0.8 V and 0.8 V in N_2 saturated PBS. The obtained cyclic voltammograms were overlaid and shown in Fig. 2 inset. As can be seen from Fig. 2 inset that maximum redox peak current was observed for 20 film deposition cycles and this optimized cycle number (20 cycles) is used for DVDR film preparation in this study. As shown in Fig. 2, during the 1st positive potential scan, the oxidation process starts at 1.6 V and a sharp oxidation peak was appeared at 2.0 V. During the consecutive cycles, an additional anodic wave appeared at 0.4 V.

The anodic peaks found at 0.4 and 1.6 V grow continuously and the corresponding oxidation peak currents increased gradually during each cycle. The peak at 1.6 V corresponds to cyanine dye monomer oxidation. Similar electrochemical behavior has been reported in literature for other cyanine dyes [30]. As reported by Lehnard *et al.*, cyanine dyes without methine chain substituents undergo rapid irreversible dimerization reaction, which is followed by deprotonation and further oxidation of the dimer which leads to an ECE-type electrode reaction resulting in the formation of a fully oxidized, tetracationic bis-dye species [31].

The small anodic wave found at 0.4 V is close to the potential of 0.43 V reported for bis-dye product formation by Lenhard *et al.* On the other hand, during the negative potential scan a sharp reduction peak was observed at -0.122 V and this reduction peak grows gradually in the consecutive cycles. However, this potential is 178 mV more positive than the potential of -0.3 V reported for the direct, irreversible reduction of the dimer tetracation [31].

Thus the above results confirmed the deposition of DVDR film on the GCE surface. Finally, the prepared DVDR/GCE was washed gently with double distilled water and utilized for the electrochemical studies.

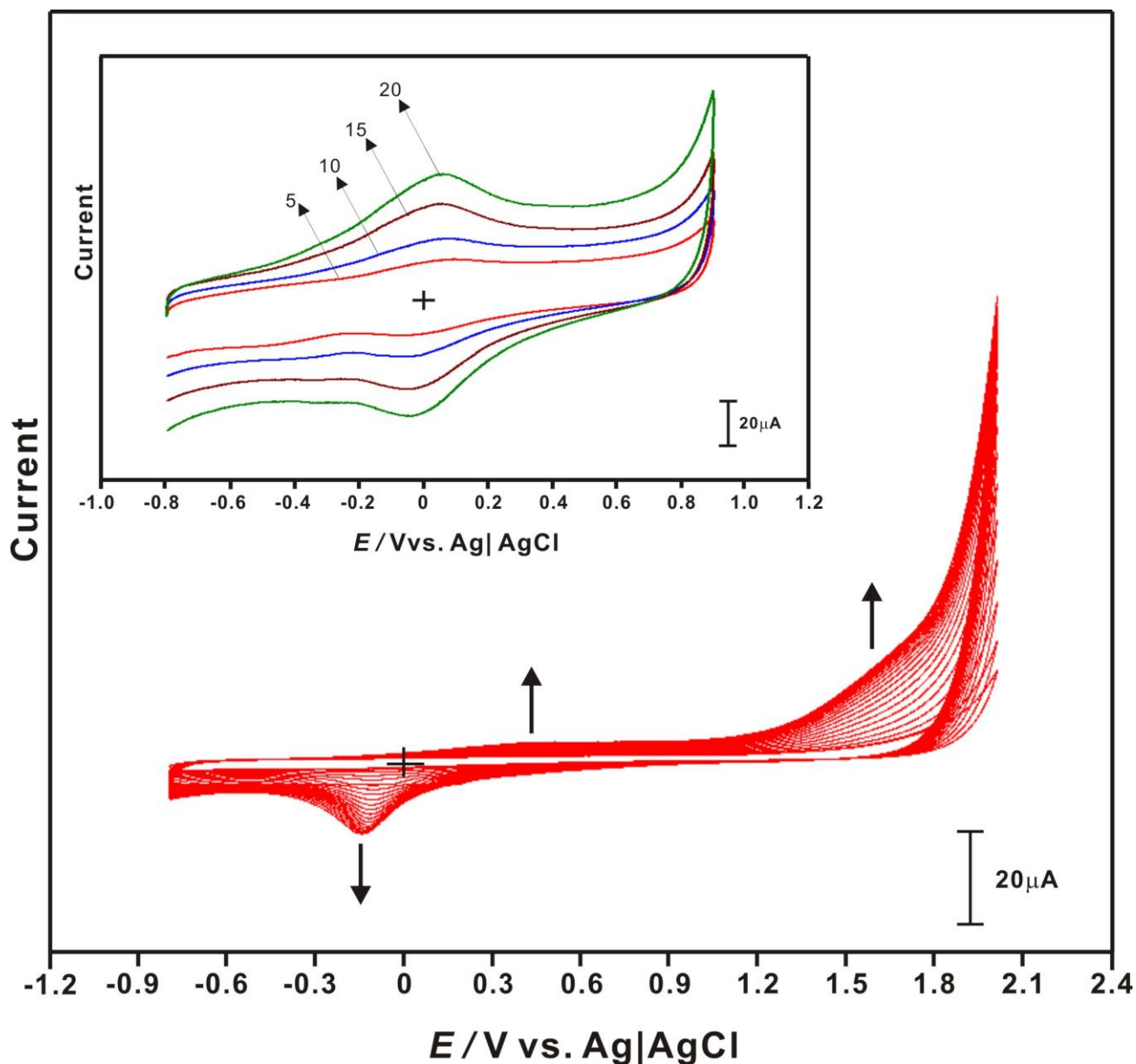


Figure 2. (a) 20 consecutive cyclic voltammograms performed at GCE in 0.1 mM DVDR dye containing 0.1 M H_2SO_4 solution. Scan rate = 100 mV s^{-1} . Inset shows the cyclic voltammograms obtained at DVDR/GCE in PBS after performing various deposition cycles.

3. RESULTS AND DISCUSSION

3.1. Electrochemical behavior of DVDR film modified GCE in PBS

Electrochemical behavior of bare/GCE and DVDR/GCE have been comparatively investigated by recording the cyclic voltammograms at the scan rate of 100 mV s^{-1} in N_2 saturated PBS. As shown in Fig. 3 (a), the unmodified GCE exhibits no redox peaks in PBS in the potential range between -0.8 V and 0.8 V. On the other hand, DVDR film modified GCE exhibits a well defined redox couple with a formal potential of 5.5 mV. This result validates the good electrochemical activity of the DVDR film.

Fig. 4 shows the cyclic voltammograms obtained at DVDR/GCE in N_2 saturated PBS at different scan rates. The peak currents (I_{pa} and I_{pc}) vs. scan rates plot shown in Fig. 4 inset exhibits a linear relationship with $R^2 = 0.999$ and 0.9997 , respectively. Both I_{pa} and I_{pc} increase linearly with increase in scan rates between 20 to 360 mV s^{-1} which validates that the redox process occurring at DVDR/GCE is surface-confined.

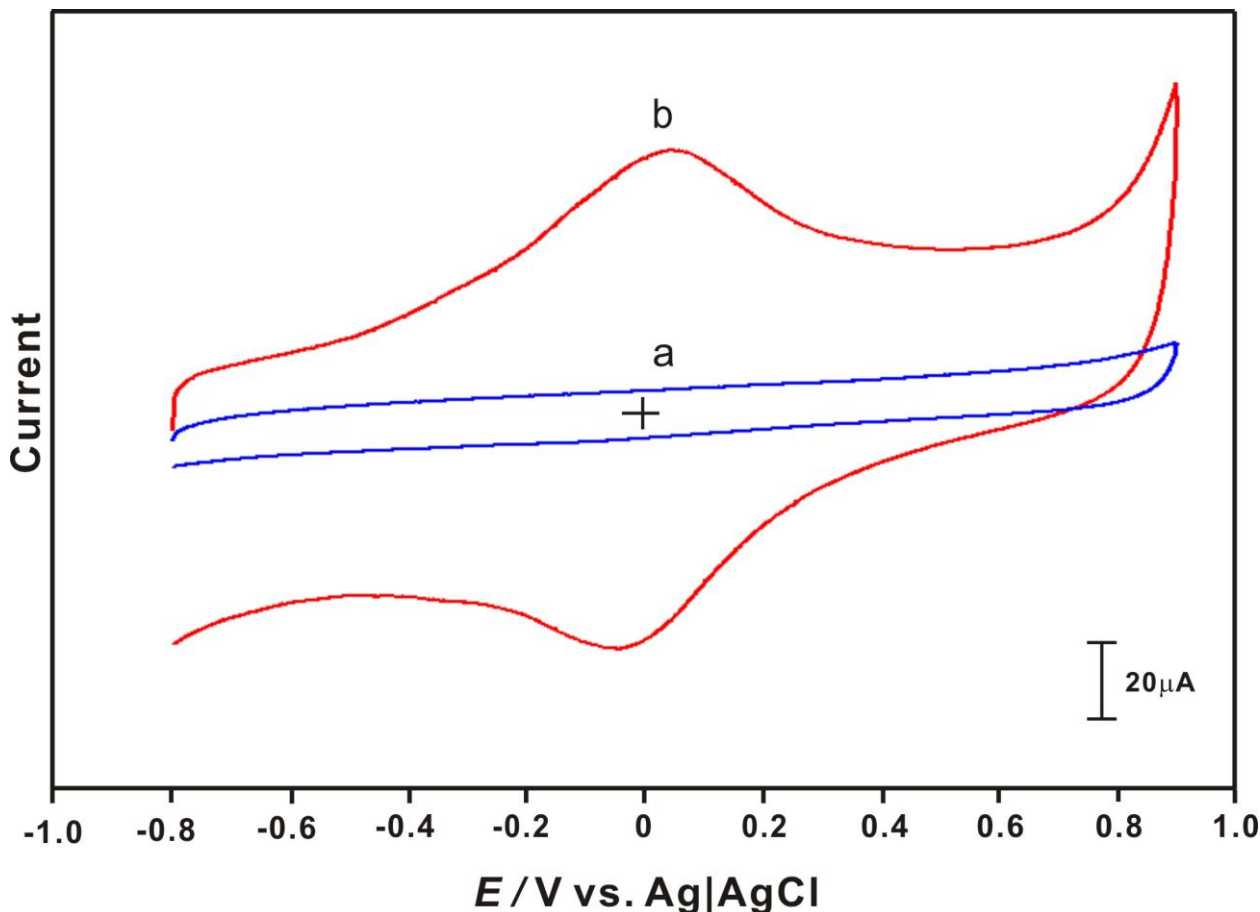


Figure 3. Cyclic voltammograms of (a) bare/GCE and (b) DVDR film modified GCE in N_2 saturated PBS at the scan rate of 100 mV s^{-1} .

As shown in Fig. 5, a pair of well-defined redox peaks has been observed at DVDR/GCE in the pH range between 1 and 13. Both I_{pa} and I_{pc} of this redox couple showed a negative shift with increase in pH. However, the peak currents decreased with increase in pH, particularly in alkaline conditions.

Since stable redox peaks were observed in pH 7 we utilized the physiological pH for the electrocatalytic experiments. Fig. 5 inset shows the linear dependence of I_{pa} , I_{pc} and $E^{o'}$ with pH. The correlation coefficient was 0.9883, respectively. From the inset plot, the slope value is calculated as 60 mV pH^{-1} which is close to the theoretical value of 56 mV pH^{-1} for equal number of proton and electron transfer process.

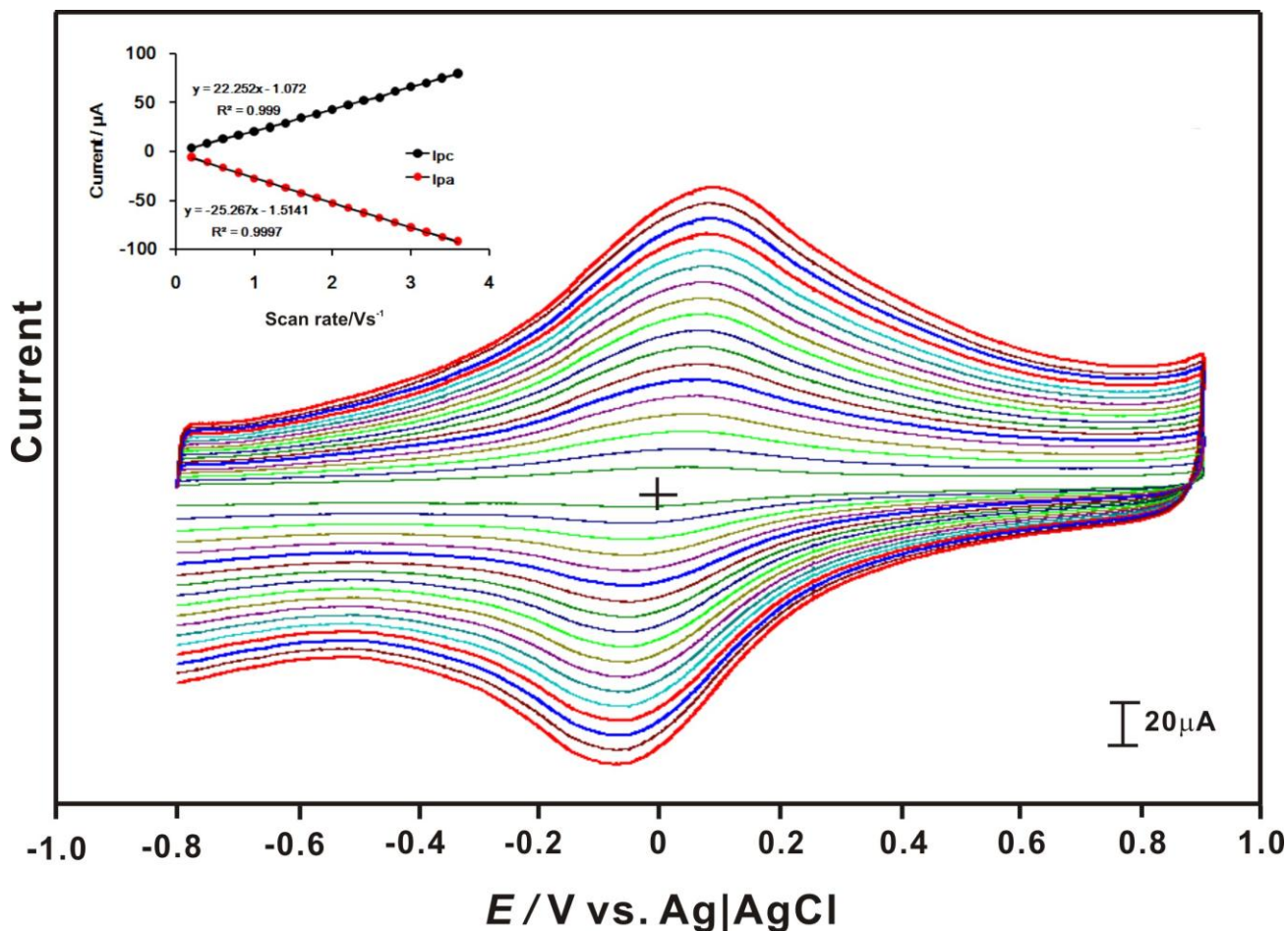


Figure 4. Cyclic voltammograms obtained at DVDR/GCE in N_2 saturated PBS at different scan rates. The scan rates from inner to outer are 20, 40, 60, 80, 100, 120, 140, 160, 180, 200, 220, 240, 260, 280, 300, 320, 340 and 360 mV^{-1} , respectively. The inset is (a) the peak currents (I_{pa} and I_{pc}) vs. scan rate/ Vs^{-1} .

3.2. Surface morphological characterizations using SEM and AFM studies

SEM study was employed to investigate the surface morphology of DVDR film. The SEM image of DVDR film at 20 μm and 10 μm magnifications are shown in Fig. 6(A) and (B). From Fig. 6(A) and (B) it is clear that a thin DVDR film has been formed on the electrode surface. The DVDR film surface displays few bead-like and elongated flake-like structures. This flake like structures could have formed due to the association of several closely deposited DVDR beads. The uniform DVDR film formed on the electrode surface validates that electrodeposition could be a more suitable technique to obtain cyanine dye thin films, as we could control the film thickness by optimizing the number of deposition cycles. In this study, 20 cycles produced a uniform thin film on the electrode surface and this optimized cycle number has been employed through out this study.

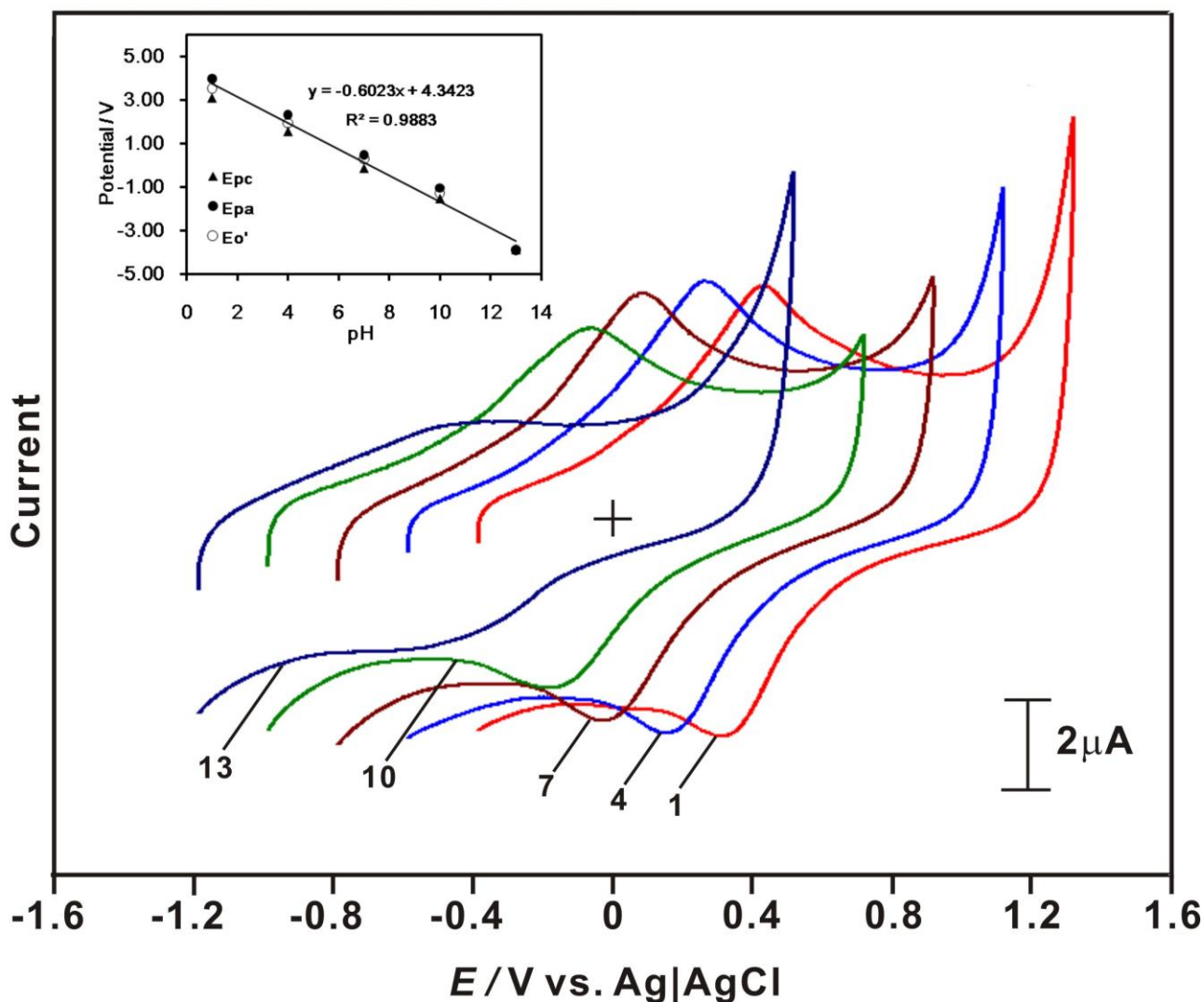


Figure 5. Cyclic voltammograms obtained at DVDR/GCE in different buffer solutions with pH: 1, 4, 7, 10 and 13, respectively. Scan rate: 100 mV s^{-1} .

Fig. 7 (a) shows the AFM image of electrochemically deposited DVDR film, where both bead-like and flake-like structures are uniformly distributed through out the film surface. The DVDR film thickness was about 290 nm. The surface morphology of the DVDR film obtained from AFM study was in good accordance with the SEM results which confirmed the efficient deposition of DVDR film.

3.3. Investigation of electrochemical behavior at the DVDR film modified electrode surface using EIS studies

Fig. 8 shows the real and imaginary parts of the impedance spectra represented as Nyquist plots (Z_{im} vs. Z_{re}) for bare/GCE and DVDR/GCE recorded in N_2 saturated PBS containing $5 \text{ mM Fe(CN)}_6^{3-/4-}$. Inset is the Randles equivalence circuit model used for fitting the EIS data of the above mentioned electrodes. From the best fitted model, we have calculated the electron transfer resistance (R_{et}), double layer capacitance (C_{dl}), Warburg impedance (W) and electrolyte resistance (R_s) values for the

unmodified and DVDR film modified GCEs. In Fig. 8, bare/GCE exhibits an enlarged semicircle with a higher R_{et} value of 1114 Ω which validates sluggish electron transfer processes. On the other hand, Nyquist plot of DVDR/GCE displays a depressed semicircle with a R_{et} value of 504.9 Ω . It is noteworthy that the R_{et} value obtained at DVDR/GCE is 2.2 fold lower than the R_{et} value observed at unmodified GCE. The smaller R_{et} value observed at DVDR film authenticates its good conductivity, which may be ascribed to the faster electron transfer resulting from the delocalization of the π -electrons present in the aromatic rings and because of the presence of conjugated double bonds in its structure.

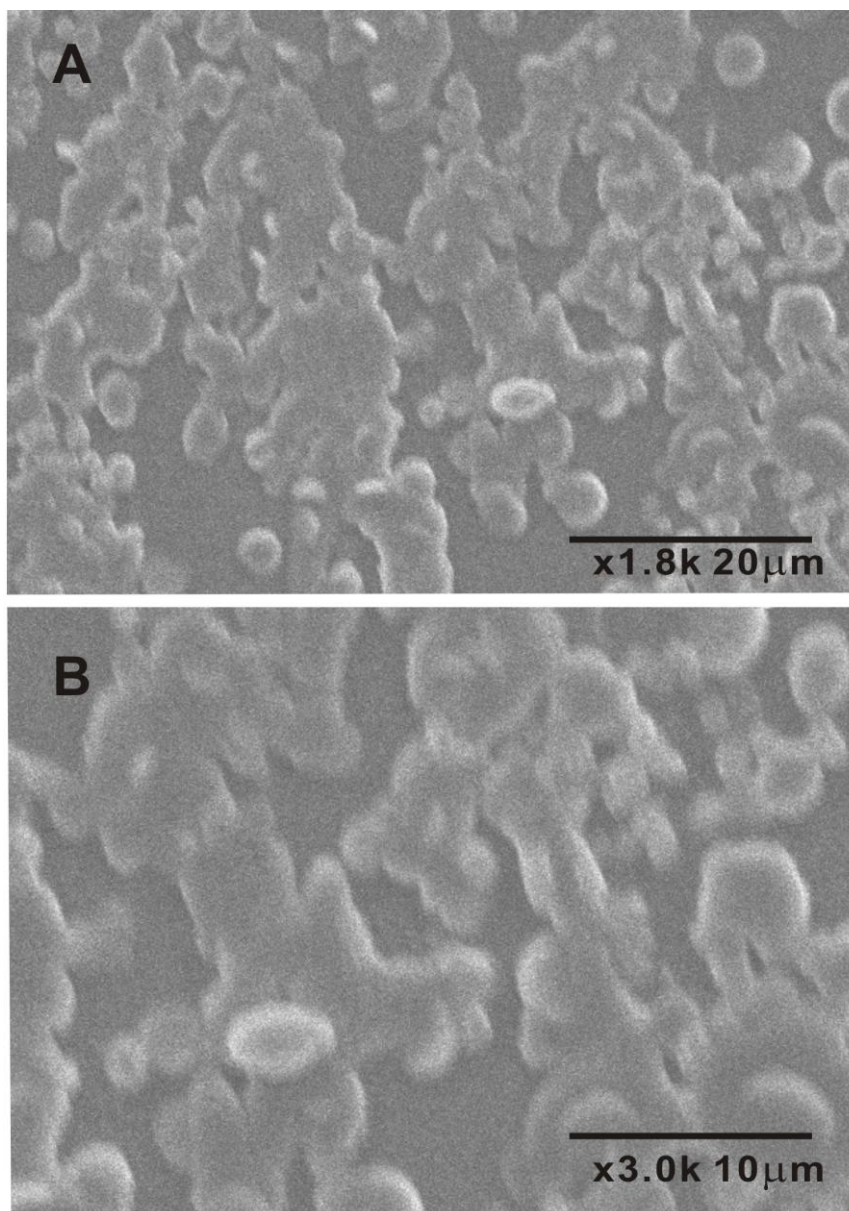


Figure 6. SEM images of DVDR film at (A) 20 μm and (B) 10 μm magnifications.

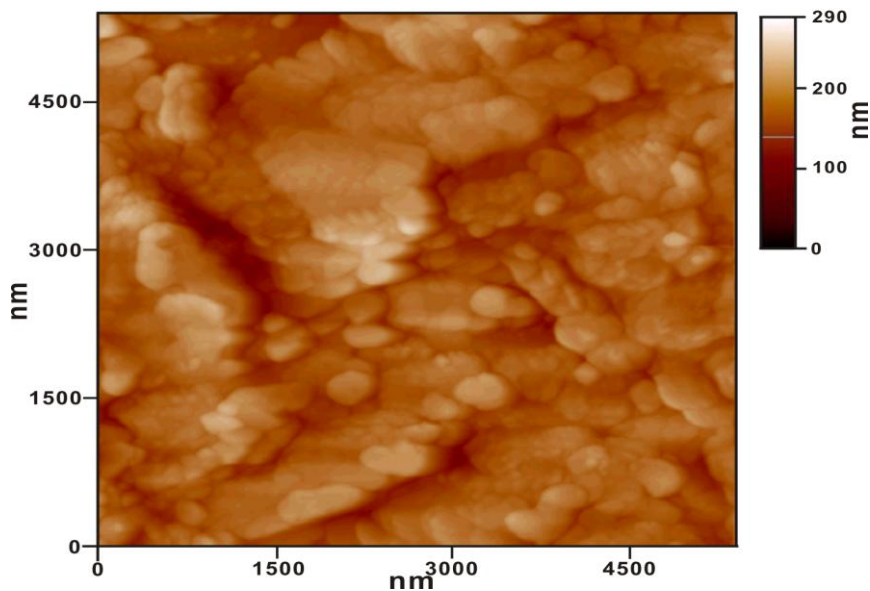


Figure 7. AFM image of DVDR film.

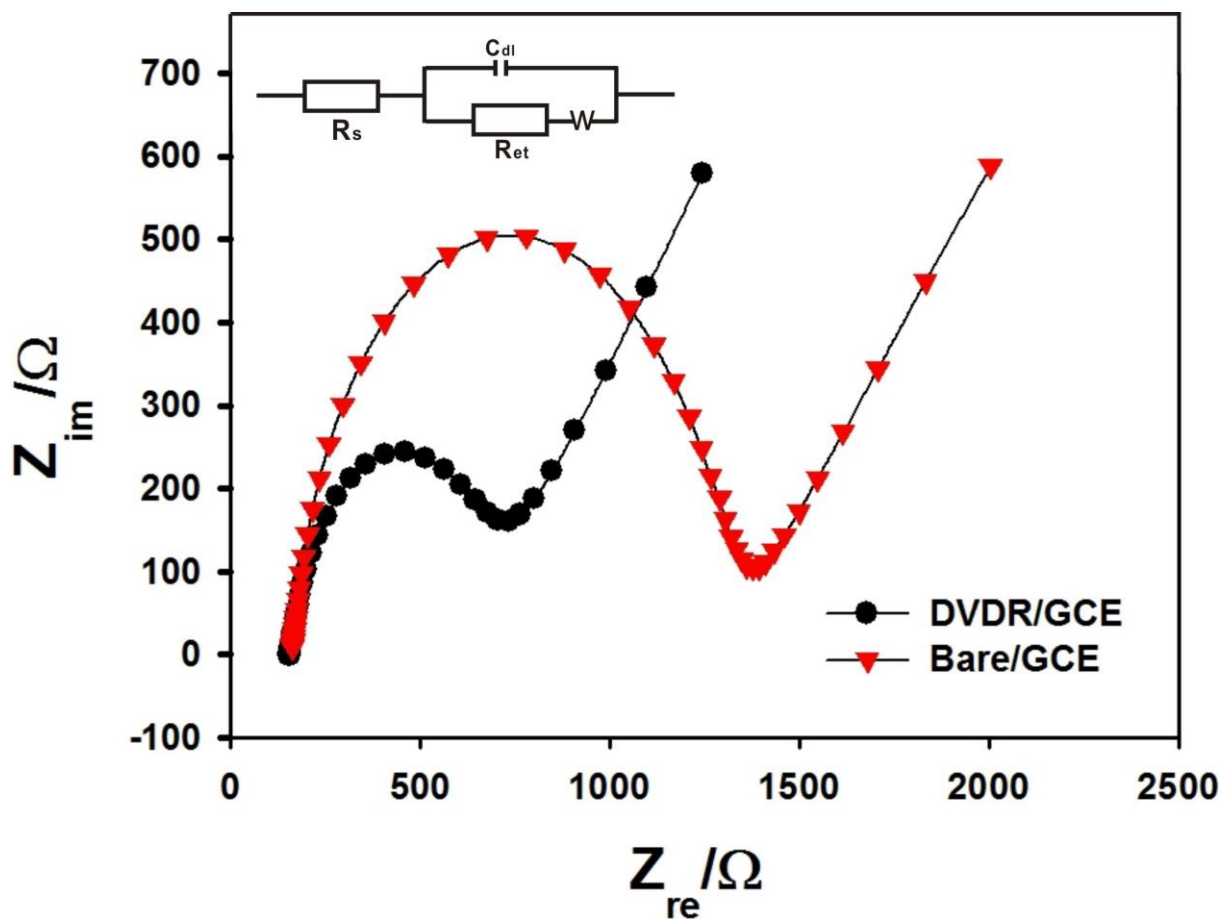


Fig. 8. EIS of bare/GCE and DVDR/GCE recorded in N_2 saturated PBS containing 5 mM $Fe(CN)_6^{3-}/Fe(CN)_6^{4-}$. Amplitude: 5 mV, frequency: 100 mHz to 100 kHz. The EIS data obtained at the bare/GCE and DVDR/GCEs were fitted using the Randles equivalence circuit given in the inset.

3.4. Impedimetric determination of hydrazine using DVDR film modified GCE

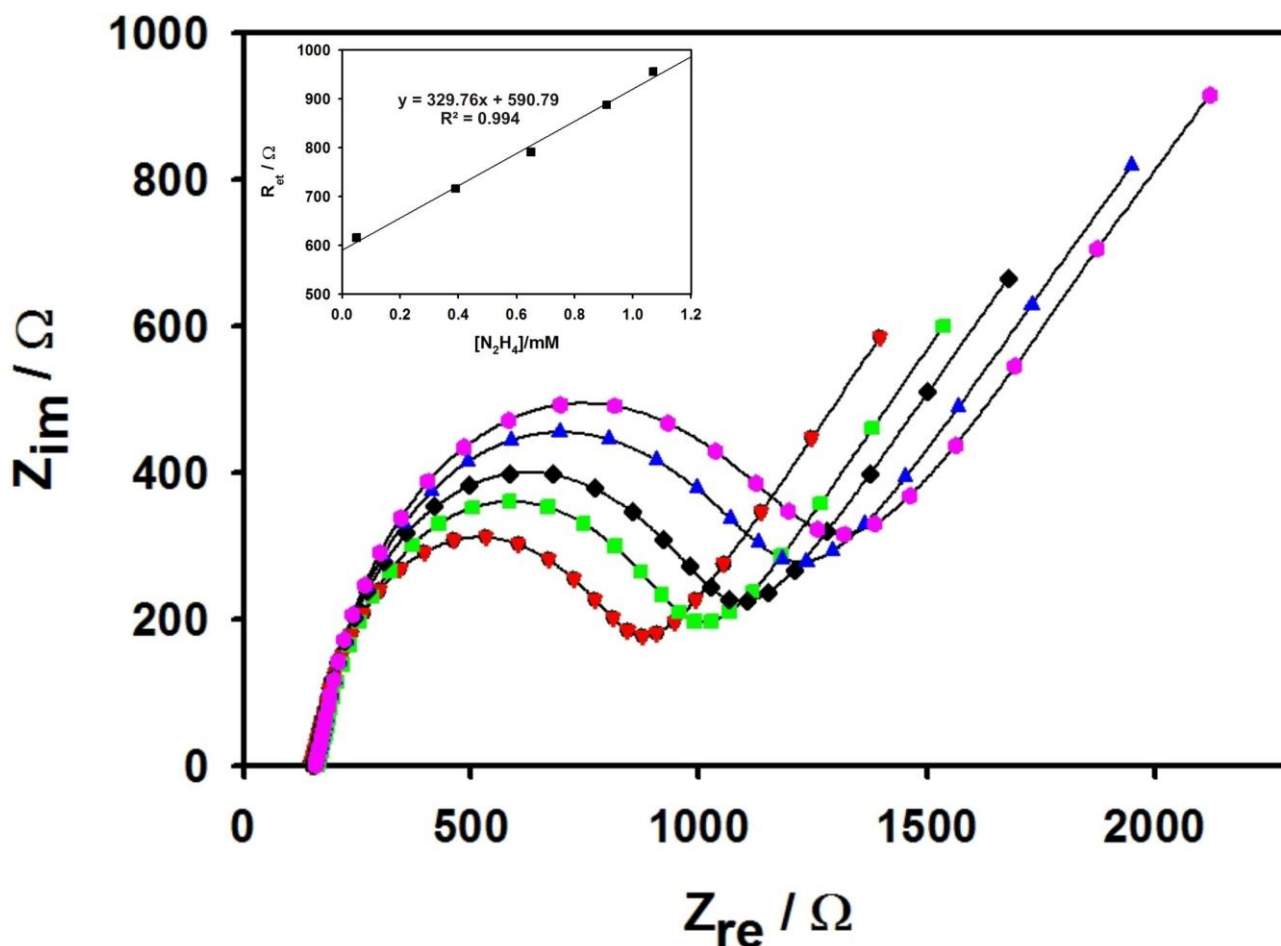


Figure 9. Impedimetric responses obtained at DVDR/GCE in the presence of various N_2H_4 concentrations in PBS containing 5 mM $Fe(CN)_6^{3-}/Fe(CN)_6^{4-}$. The Nyquist plots from inner to outer were obtained after successive addition of 0.05 mM, 0.39 mM, 0.65 mM, 0.91 mM and 1.07 mM N_2H_4 concentrations into the supporting electrolyte solution. Amplitude: 5 mV, frequency: 100 mHz to 100 kHz.

In order to develop an impedimetric biosensor for hydrazine quantification, we performed EIS measurements at DVDR/GCE in the presence of various N_2H_4 concentrations in PBS containing 5 mM $Fe(CN)_6^{3-}/Fe(CN)_6^{4-}$. The obtained Nyquist plots are shown in Fig. 9. The semicircles from inner to outer are the impedimetric responses obtained at DVDR/GCE for 0.05 mM–1.07 mM N_2H_4 concentration additions. It is clear that the semicircle diameter is increasing with increase in N_2H_4 concentration additions. Similar results have been reported at other impedimetric sensors developed for glutamate [32] and Uranyl ion (UO_2^{2+}) determinations [33], in which they observed an increase in semicircle diameter while increasing glutamate and UO_2^{2+} concentrations, respectively. In the present study, the reason for the augmentation in semicircle diameter with increase in N_2H_4 concentrations could be attributed to the insulation layer formed by the adsorbed N_2H_4 at modified electrode surface, which inhibits the charge transfer for the redox probe. By fitting the obtained experimental data with

the Randles equivalence circuit, the R_{ct} values have been calculated. As shown in Fig. 9 inset, a calibration curve was obtained by plotting the R_{ct} values against the added N_2H_4 concentrations. From this calibration plot, the linear concentration range, correlation coefficient and sensitivity values are calculated as 0.05 mM–1.07 mM, 0.994 and $4.174 \text{ K}\Omega \text{ mM}^{-1} \text{ cm}^{-2}$, respectively. The good impedimetric hydrazine detection results achieved at the DVDR/GCE could be attributed to the good affinity of the composite film towards hydrazine.

3.5. Electrocatalytic oxidation of hydrazine at DVDR film modified GCE

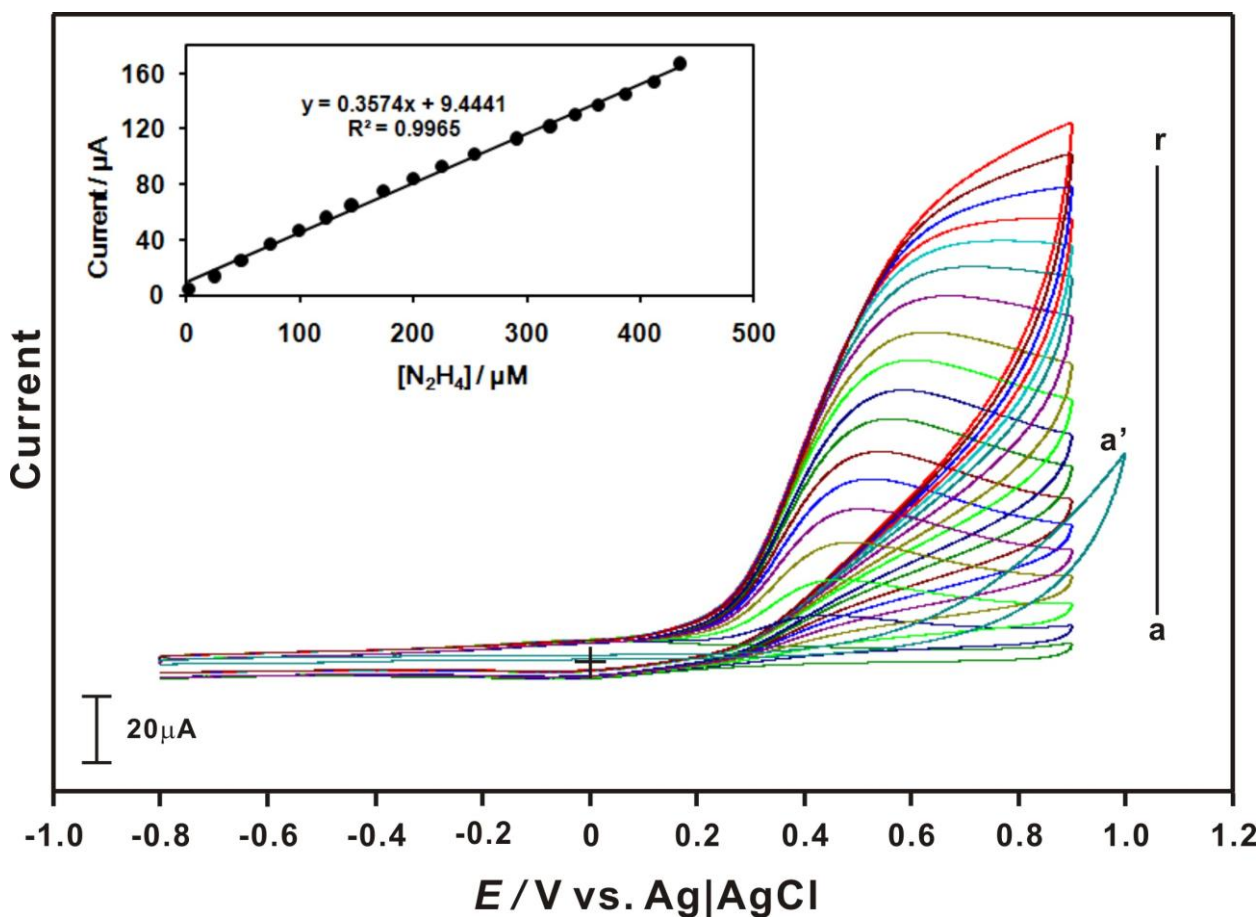


Figure 10. Cyclic voltammograms obtained at DVDR film modified GCE at the scan rate of 100 mV s^{-1} in the presence of: (a) 0.02, (b) 0.25, (c) 0.48, (d) 0.74, (e) 1.0, (f) 1.23, (g) 1.45, (h) 1.74, (i) 2.0, (j) 2.25, (k) 2.54, (l) 2.91, (m) 3.20, (n) 3.42 (o) 3.63 (p) 3.87 (q) 4.12 and (r) 4.35 mM hydrazine in PBS. (a') cyclic voltammogram obtained at the bare/GCE in the presence of 4.35 mM hydrazine. The supporting electrolyte is N_2 saturated PBS. Inset is the plot of anodic peak current vs. $[\text{hydrazine}] = [N_2H_4]$.

The electrocatalytic activity of DVDR film modified GCE towards hydrazine oxidation has been investigated in this study owing to the good conductivity and synergistic effect of DVDR film towards hydrazine. Fig. 10(a-r) shows the cyclic voltammograms obtained at DVDR/GCE for various N_2H_4 concentration additions. As shown in Fig. 10 (a) when 0.02 mM of N_2H_4 was injected into the

PBS, the DVDR film exhibits a well-defined oxidation peak at 0.38 V corresponding to the N_2H_4 oxidation. Since then the oxidation peak current increased linearly with increase in N_2H_4 concentration additions (see Fig. 10 (b-r)). The DVDR film thus exhibits promising electrocatalytic activity towards N_2H_4 . On the other hand, no obvious N_2H_4 oxidation peak was observed at the bare/GCE even in the presence of 4.35 mM N_2H_4 and further it requires much higher potential to reduce N_2H_4 , which signifies that bare/GCE has no catalytic activity for N_2H_4 . Here it is noteworthy that, DVDR/GCE has decreased the over potential for N_2H_4 oxidation which validates the excellent electrocatalytic activity of the DVDR film. Fig. 10 inset shows the calibration plot of linear dependence of I_{pa} with various N_2H_4 concentrations. From this calibration plot, the linear concentration range is obtained as 20 μM -4.4 mM and the sensitivity is $4.524 \mu A mM^{-1} cm^{-2}$ of hydrazine, respectively.

3.6. Amperometric determination of hydrazine at DVDR film modified rotating GCE

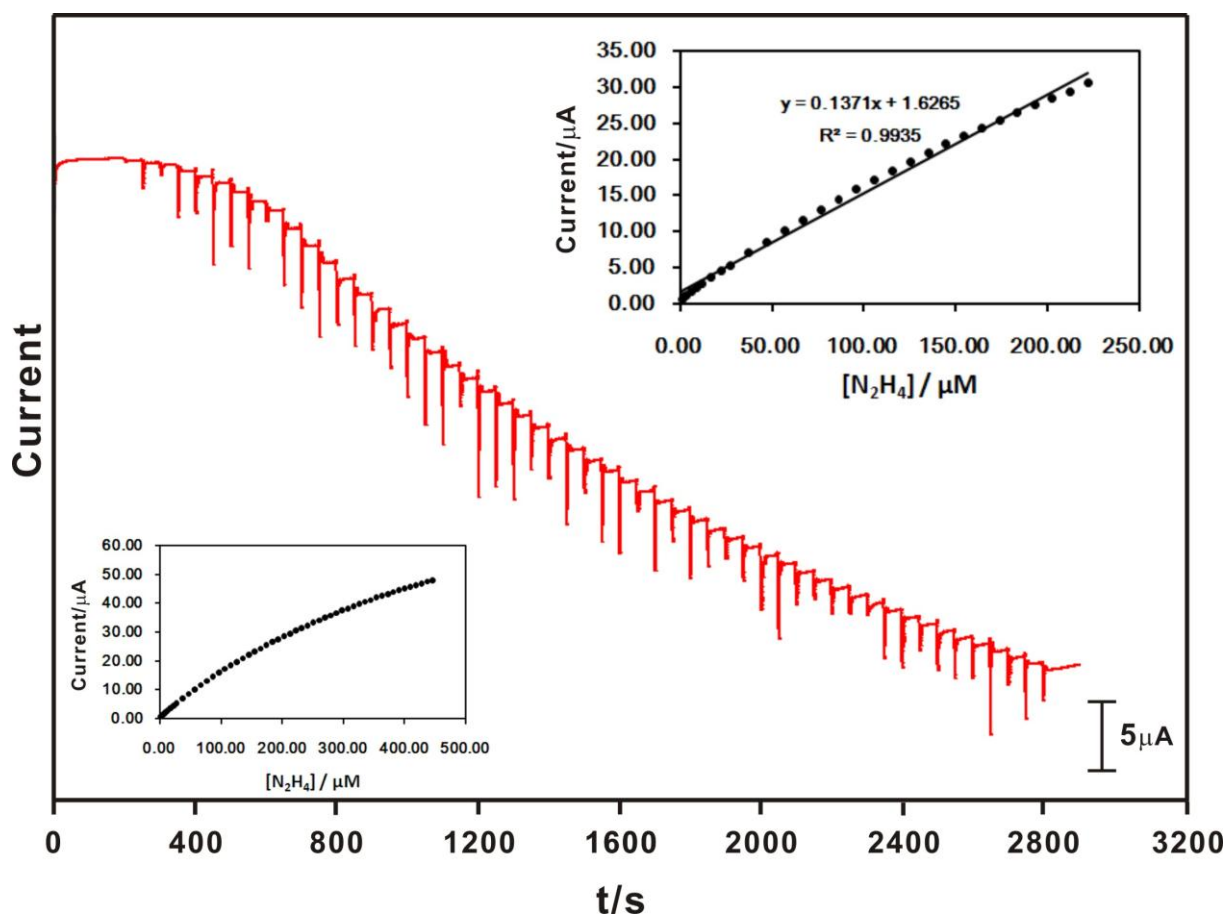


Figure 11. (A) Amperometric $i-t$ response at DVDR film modified rotating disc GCE upon successive additions of $1 \times 10^{-6} M$ to $4.46 \times 10^{-4} M$ N_2H_4 into continuously stirred 100 ml N_2 saturated PBS. Applied potential: 0.5 V; Rotation rate: 1200 RPM. The lower inset is the plot of linear dependence of peak current vs. $[N_2H_4]/\mu M$. The N_2H_4 concentration range used was between $1 \times 10^{-6} M$ to $4.46 \times 10^{-4} M$ N_2H_4 , respectively. The upper inset is the linear calibration plot obtained for $1 \times 10^{-6} M$ and $2.22 \times 10^{-4} M$ N_2H_4 concentration additions.

Fig. 11 (A) shows the amperometric *i-t* curve recorded at DVDR film modified rotating disc GCE in 100 ml N₂ saturated PBS. The electrode potential was held at 0.5 V. For every 50 s, aliquots of N₂H₄ were successively injected into the supporting electrolyte solution. It is clear that, for each N₂H₄ concentration additions, the DVDR film showed rapid, well-defined amperometric response. The increase in steady state current corresponds to the oxidation of hydrazine. In Fig. 11, the lower inset shows the dependence of catalytic response current with various N₂H₄ concentration additions. The upper inset shows the calibration plot obtained for 1 × 10⁻⁶ M–2.22 × 10⁻⁴ M N₂H₄ concentration additions. The linear hydrazine concentration range detected at DVDR film in this study is higher than the linear hydrazine concentration range reported at other modified electrodes [34–38]. From this calibration plot, the correlation coefficient and sensitivity values are obtained as 0.9935 and 0.571 μA μM⁻¹ cm⁻² of hydrazine, respectively. The good linear range and high sensitivity obtained at the DVDR film validates this trimethine cyanine dye film as a good candidature for hydrazine sensor.

3.7. Investigation of the selectivity of the DVDR film towards hydrazine oxidation

As several common cations/anions coexist with hydrazine in nature, the study of the influence of the interfering ions on the hydrazine determination is mandatory. In this study, the selectivity of the prepared DVDR film modified rotating GCE was investigated in the presence of various cations and anions using amperometric *i-t* curve study. The results are shown in Fig. 12. The amperometric experimental conditions are same as that mentioned in Fig. 11.

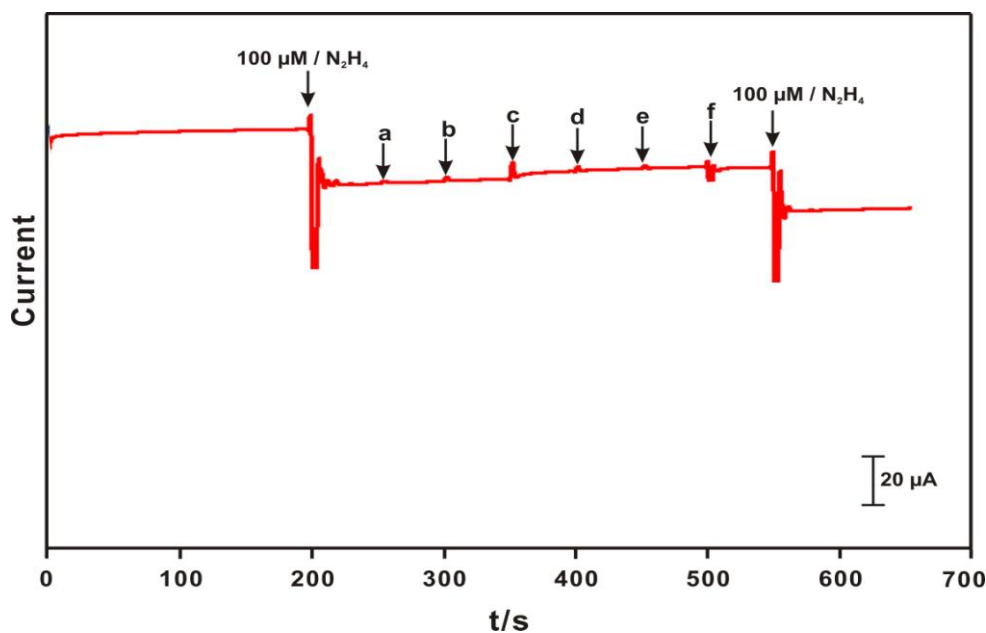


Fig. 12. Amperometric *i-t* response at DVDR film modified rotating disc GCE for successive additions of (a) 1 M NO₃⁻, (b) 1 M SO₄²⁻, (c) 1 M Ca²⁺, (d) 1 M K⁺, (e) 0.5 M Na⁺ and (f) 0.5 M I⁻ species containing solutions into continuously stirred N₂ saturated PBS. Well-defined amperometric responses observed at 200s and 550 s were obtained for 100 μM N₂H₄ additions into the same supporting electrolyte solution. The applied potential: 0.5 V; Rotation rate: 1200 RPM.

In Fig. 12, the DVDR film modified rotating GCE shows a rapid, well-defined amperometric response at 200 s for 100 μM N_2H_4 additions. As shown in Fig. 12 (a-f), no notable amperometric responses were observed at the DVDR/GCE when 1 M NO_3^- , 1 M SO_4^{2-} , 1 M Ca^{2+} , 1 M K^+ , 0.5 M Na^+ and 0.5 M I^- species were successively injected into the same PBS. However, a well-defined amperometric response was observed at 550 s, when 100 μM N_2H_4 was injected into the same supporting electrolyte solution. Even though when large amounts (1000/500 fold) of the above mentioned cations/anions were coexisting with hydrazine in the same supporting electrolyte solution, they doesn't offer any interfere effect to the hydrazine oxidation signal appearing at the DVDR film, which validates the high selectivity of the DVDR film towards hydrazine oxidation.

3.8. Determination of hydrazine from various spiked water samples

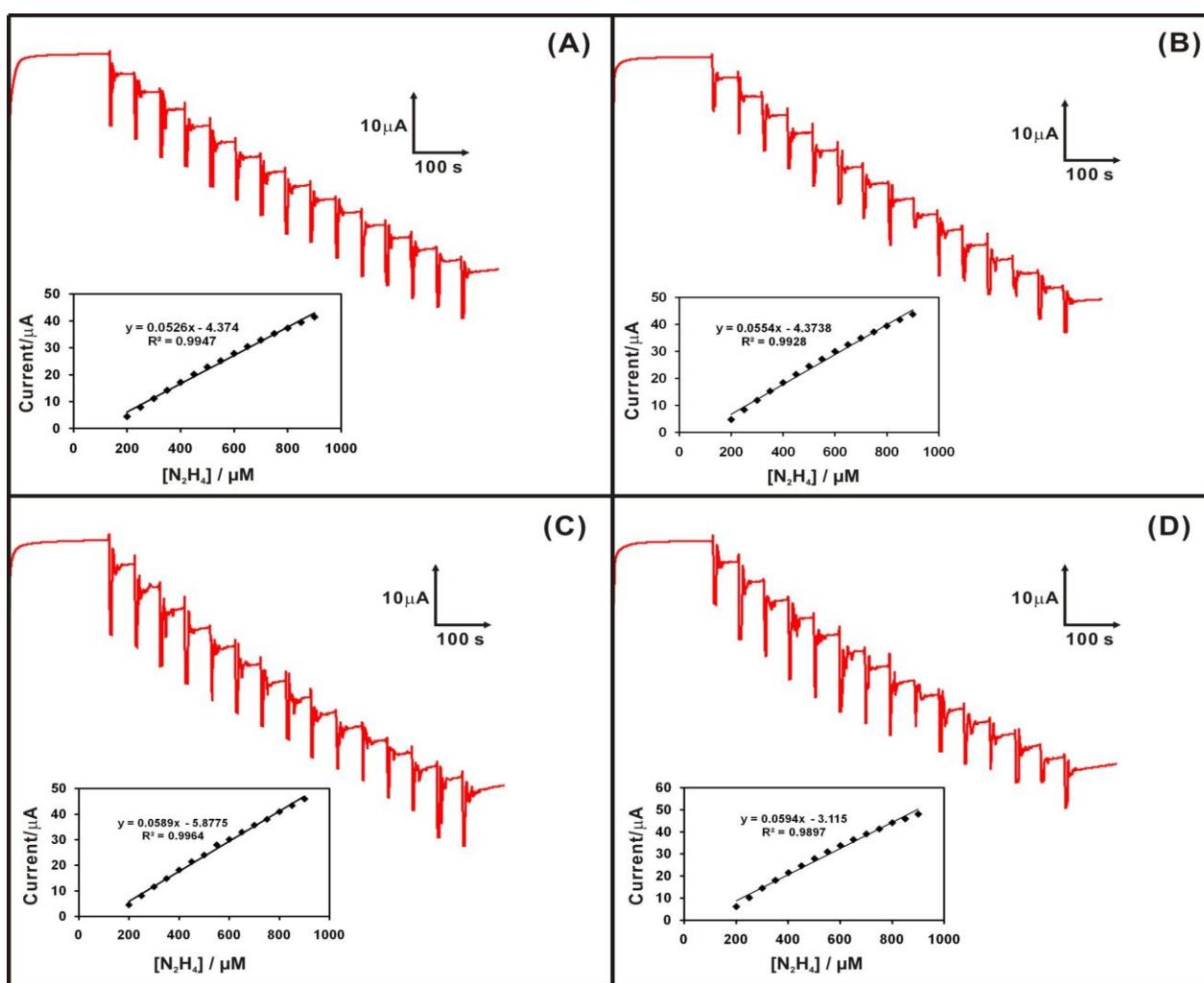


Fig. 13 (A–D) Amperometric *i-t* responses obtained at DVDR film modified rotating disc GCE for each 50 μM N_2H_4 concentrations (15 successive additions) spiked into the continuously stirred 100 ml N_2 saturated PBS, distilled water, tap water and pond water samples, respectively. The spiked N_2H_4 concentrations were between $2.5 \times 10^{-4}\text{M}$ and $9 \times 10^{-4}\text{M}$, respectively. Applied potential: 0.5 V; Rotation rate: 1200 RPM. The insets are the calibration plots for the linear dependence of anodic peak current vs. $[\text{N}_2\text{H}_4] / \mu\text{M}$.

The determination of hazardous chemicals in water samples is obligatory and it could be achieved by electrochemical methods using standard addition method [39, 40]. Recently, excellent recovery of hydrazine from water and urine samples have been reported by several research groups using voltammetric techniques [38, 41, 42]. In this study, we attempted to evaluate the practical applicability of the DVDR/GCE towards hydrazine determination using amperometric technique. During amperometric measurements, 50 μM N_2H_4 (15 successive additions) was spiked into continuously stirred N_2 saturated PBS, distilled water, tap water and pond water samples. The results are shown in Fig. 13 (A)–(D). It is clear from Fig. 13 (A), well-defined amperometric responses were observed at the DVDR film for all 15 successive (50 μM N_2H_4 each) additions into the PBS which reveals the excellent electrocatalytic activity of DVDR film. From the inset calibration plot the linear concentration range, correlation coefficient and sensitivity values are obtained as $2.5 \times 10^{-4}\text{M}$ – $9 \times 10^{-4}\text{M}$, 0.9947 and $0.219 \mu\text{A} \mu\text{M}^{-1} \text{cm}^{-2}$, respectively. Similarly, as shown in Fig. 13 (B-D), for all 50 μM N_2H_4 concentrations additions, well defined amperometric responses were obtained in distilled water, tap water and pond water samples with a good linear concentration range between $2.5 \times 10^{-4}\text{M}$ and $9 \times 10^{-4}\text{M}$. The correlation coefficient and sensitivity values are 0.9928, 0.9964 and 0.9897 and 0.231, 0.245, $0.246 \mu\text{A} \mu\text{M}^{-1} \text{cm}^{-2}$, respectively. From the amount of spiked and found hydrazine concentrations the average recovery (%) was calculated. The average recovery (%) for hydrazine in distilled water, tap water and pond water samples are 94, 97 and 79 %, respectively. The low average recovery (%) obtained in the spiked pond water sample might be due to the reason that the impurities present in the pond water may altered the hydrazine quantification signal, as we utilized the pond water sample for our analysis without any filtration. The determination of N_2H_4 from spiked water samples with acceptable average recovery (%) shows the practical applicability of the proposed method.

4. CONCLUSIONS

A highly selective amperometric and impedimetric sensor for hydrazine has been developed using a novel trimethine cyanine dye, DVDR film modified glassy carbon electrode. The DVDR film surface exhibits excellent catalytic activity towards hydrazine, which could be ascribed to the synergistic effect of the dye film for hydrazine. The developed hydrazine sensor, successfully detects hydrazine spiked into various water samples with acceptable recovery. The proposed method possesses advantages like preparation of trimethine cyanine dye thin films on carbon electrode surface in short time, effortless electrodeposition technique, green approach, and its good catalytic activity towards electrochemically active hazardous compound such as hydrazine. Thus the present study may encourage the utilization of this dye for the selective detection of other hazardous chemicals present in industrial effluents. The thin film forming ability of this class of dyes revealed in the present study may thus promote their use in the fabrication of other energy storage devices such as dye-sensitized solar cell and fuel cells.

ACKNOWLEDGEMENT

This work was supported by the National Science Council and the Ministry of Education of Taiwan (Republic of China).

References

1. D.L. Akins, V.T. Kumar, *J. Chromatogr. A*, 689 (1995) 269.
2. K. C. Hannah, B. A. Armitage, *Acc. Chem. Res.*, 37 (2004) 845.
3. T. G. Deligeorgiev, D. A. Zaneva, H. E. Katerinopoulos, V. N. Kolev, *Dyes Pigm.*, 41 (1999) 49.
4. K. Meguellati, G. Koripelly, S. Ladame, *Angew. Chem. Int. Ed.*, 49 (2010) 2738.
5. J. Bricks, A. Ryabitskii, A. Kachkovskii, *Chem. Eur. J.*, 16 (2010) 8773.
6. S. J. Mason and S. Balasubramanian, *Org. Lett.*, 4 (2002) 4261.
7. Q. Li, J. Tan, B. X. Peng, *Molecules*, 2 (1997) 91.
8. F. M. Eissa, *J. Chin. Chem. Soc.*, 56 (2009) 843.
9. H. S. Rye, S. Yue, D. E. Wemmer, M. A. Quesada, R. P. Haugland, R. A. Mathies, A. N. Glazer, *Nucleic Acids Res.*, 20 (1992) 2803.
10. M. Lu, Q. Guo, N. C. Seeman, N. R. Kallenbach, *Biochemistry*, 29 (1990) 3407.
11. J. Tang, W. Wu, J. Hua, J. Li, X. Li, H. Tian, *Energy Environ. Sci.*, 2 (2009) 982.
12. W. J. Wu, W.H. Zhan, J.L. Hua, H. Tian, *Res. Chem. Intermed.*, 34 (2008) 241.
13. J. P. Hermann, *Optics Communications*, 12 (1974) 102.
14. G. Mchale, M. I. Newton, P. D. Hooper, M. R. Willis, *Opt. Mater.*, 6 (1996) 891.
15. Z. Hong Peng, H. J. Geise, X. F. Zhou, B. X. Peng, R. Carleer, R. Dommissie, *Liebigs Ann. Recl.*, 27 (1997).
16. T. L. Netzel, K. Nafisi, M. Zhao, *J. Phys. Chem.* 99 (1995) 17936.
17. J. E. Troyan, *Industrial and Engineering Chemistry*, 45 (1953) 2609.
18. N. V. Rees, R. G. Compton, *Energy Environ. Sci.*, 4 (2011) 1255.
19. M. M. Ardakani, M. A. Karimi, M. M. Zare, S. M. Mirdehghan, *Int. J. Electrochem. Sci.*, 3 (2008) 246.
20. J. B. Raoof, R. Ojani, M. Ramine, *Electroanal.*, 19 (2007) 597.
21. M. Sun, L. Bai, D. Q. Liu, *J. Pharm. Biomed. Anal.*, 49 (2009) 529.
22. M.I. Evgenyev, S. Y. Garmonov, I. I. Evgenyeva, H. C. Budnikov, *Talanta*, 42 (1995) 1465.
23. H. R. Zare, N. Nasirizadeh, *Electroanal.*, 18 (2006) 507.
24. K. I. Ozoemena, *Sensors*, 6 (2006) 874.
25. H. Razmi, A. Azadbakht, M. H. Sadr, *Anal. Sci.*, 21 (2005) 1317.
26. M. M. Ardakani, H. Rajabi, B. B. F. Mirjalili, H. Beitollahi, A. Akbari, *J. Solid State Electrochem.*, 14 (2010) 2285.
27. S. M. Chen, M. H. Wu, R. Thangamuthu, *Electroanal.*, 20 (2008) 178.
28. S. M. Chen, M. F. Lu, K. C. Lin, *Electroanal.*, 17 (2005) 847.
29. Y. Umasankar, T. Y. Huang, S. M. Chen, *Anal. Biochem.*, 408 (2011) 297.
30. J. L. Lyon, D. M. Eisele, S. Kirstein, J. P. Rabe, D. A. V. Bout, K. J. Stevenson, *J. Phys. Chem. C*, 112 (2008) 1260.
31. J. R. Lenhard, A. D. Cameron, *J. Phys. Chem.*, 97 (1993) 4916.
32. R. Maalouf, H. Chebib, Y. Saikali, O. Vittori, M. Sigaud, N. J. Renault, *Biosens. Bioelectron.*, 22 (2007) 2682.
33. R. K. Shervedani, S. A. Mozaffari, *Anal. Chim. Acta*, 562 (2006) 223.
34. S. V. Guerra, L.T. Kubota, C. R. Xavier, S. Nakagaki, *Anal. Sci.*, 15 (1999) 1231.
35. H. Zhang, J. Huang, H. Hou, T. You, *Electroanal.*, 21 (2009) 1869.
36. J. Liu, Y. Li, J. Jiang, X. Huan, *Dalton Trans.*, 39 (2010) 8693.
37. H. Yang, B. Lu, L. Guo, B. Qi, *J. Electroanal. Chem.*, 650 (2011) 171.
38. J. B. Raoof, R. Ojani, Z. Mohammadpour, *Int. J. Electrochem. Sci.*, 5 (2010) 177.

39. M. M. Ardakani, Z. Taleat, *Int. J. Electrochem. Sci.*, 4 (2009) 694.
40. G. A. M. Mersal, *Int. J. Electrochem. Sci.*, 4 (2009) 1167.
41. M. R. Akhgar, M. Salari, H. Zamani, A. Changizi, H. H. Mahdiabad, *Int. J. Electrochem. Sci.*, 5 (2010) 782.
42. N. Rastakhiz, A. Kariminik, V. S. Nejad, S. Roodsaz, *Int. J. Electrochem. Sci.*, 5 (2010) 1203.